

The efficiency of gamma-ray emission from pulsars

Bronisław Rudak¹, Jarosław Dyks²

¹*N. Copernicus Astronomical Center, Rabiańska 8, 87-100 Toruń, Poland*

e-mail: bronek@camk.edu.pl

²*Dept. of Physics and Astronomy, UMK, Grudziądzka 5/7, 87-100 Toruń, Poland*

e-mail: jinx@astri.uni.torun.pl

in the press

ABSTRACT

We present a modified scenario of gamma-ray emission from pulsars within the framework of polar cap models. Our model incorporates possible acceleration of electron-positron pairs created in magnetospheres, and their subsequent contribution to gamma-ray luminosity L_γ . It also reproduces the empirical trend in L_γ for seven pulsars detected with *Compton Gamma Ray Observatory* (*CGRO*) experiments. At the same time it avoids basic difficulties (Nel et al. 1996, Arons 1996) faced by theoretical models when confronted with observational constraints.

We show that the classical and millisecond pulsars form two distinct branches in the $L_\gamma - L_{\text{sd}}$ diagram (where L_{sd} is the spin-down luminosity). In particular, we explain why the millisecond pulsar J0437-4715 has not been detected with any of the *CGRO* instruments despite its very high position in the ranking list of spin-down fluxes (i.e. L_{sd}/D^2 , where D is a distance). The gamma-ray luminosity predicted for this particular object is about one order of magnitude below the upper limit set by *EGRET*.

Key words: gamma-rays: theory, observations – pulsars: general

1 INTRODUCTION

Numerous models of pulsars (see Michel 1991 for the review) proposed over the last three decades tried to make specific predictions about emission of gamma-rays and X-rays. Gamma-rays are particularly important as a direct signature of basic non-thermal processes in pulsar magnetospheres, and potentially should help to discriminate among different models. Interpreting gamma-rays should also be less ambiguous compared to X-rays. In the latter case, especially for objects younger than 10^6 yr, contributions from initial cooling, internal friction, etc. of unknown magnitude may dominate the total X-ray emission.

There are seven positive detections of pulsars by *CGRO* (see Table 1), i.e. less than one per cent of all pulsars known to date. In all cases the sources had been identified by virtue of gamma-ray flux modulations with previously known *P. Crab* and *Vela* are the only pulsars seen by three of *CGRO* detectors.

The *EGRET* data became so far the only ground for testing theoretical models. The latest critical review of three models of gamma-ray emission (polar cap models by Harding 1981, Dermer & Sturmer 1994, and outer gap model of Yadigaroglu & Romani 1995) comes from Nel et al.(1996). They conclude that none of the models fits observations satisfactorily for two major reasons. First, the confrontation

of polar cap models (Harding 1981, and Dermer & Sturmer 1994) with the observations leads to a relation

$$L_\gamma(\text{observ.}) \propto L_\gamma^\alpha(\text{model}), \quad (1)$$

with $\alpha \simeq 0.6$ and 0.5 , respectively, instead of $\alpha = 1$. Second, there have always been some cases amongst ~ 350 *EGRET* upper limits, apparently contradicting predictions of L_γ made by the models. The troublesome limits come usually from the pulsars B1509-58, B1046-58, B0656+14, B1929+10, B0950+08, as well as from the millisecond object J0437-4715.

Of these two problems raised by Nel et al.(1996), the latter is more severe in our opinion. The former problem may be solved to some degree by updating parameters used for two objects at the low-luminosity domain, i.e. B1055-52 and Geminga. After Thompson et al.(1994), Nel et al. used for B1055-52 the spectral index $\gamma = 1.18$ determined by Fierro et al. (1993) from the first three viewing periods of *EGRET*. However, a substantially higher value, $\gamma = 1.59$, based on the data from 10 viewing periods became recently available (Fierro 1995). This value of the spectral slope reduces L_γ of B1055-52 by a factor of ~ 4 . (We shall discuss other consequences of the steeper spectral slope for B1055-52 in Section 3). Further reduction of L_γ in the case of B1055-52 is possible by lowering distance D to the source. The argument for lowering the distance (the usually assumed value

Table 1. Gamma-ray luminosities for pulsars detected with *CGRO* (in log of [erg s⁻¹]). Beaming angle of emission $\Omega_\gamma = 1$ sr was assumed.

PSR		log L_{sd}	<i>EGRET</i>	<i>COMPTEL</i>	<i>OSSE</i>	Refs.	'total'
B0531+21	Crab	38.65	34.6	35.0	35.1	1,2,3	35.42
B1509-58		37.25	–	–	34.4	-, -, 3	34.40
B0833-45	Vela	36.84	34.2	33.5	31.3	1,2,3	34.28
B1951+32		36.57	34.1	34.1	–	1,4,-	34.40
B1706-44		36.53	34.4	–	–	1,-,-	34.40
J0633+1746	Geminga*	34.51	32.9	+	–	1,5,-	32.90
B1055-52		34.48	33.4	–	–	6,-,-	33.40

*at the distance of 157 pc.

Refs. to flux values:

- 1) Ramanamurthy et al.(1995), 2) Carramiñana et al.(1995), 3) Schroeder et al.(1995),
 4) Kuiper et al.(1996a), 5) Kuiper et al.(1996b), 6) Fierro (1995)

is 1.53 kpc, after the model of Taylor & Cordes 1993) may come from *ROSAT* PSPC observations. If the bulk of the (presumably) thermal X-ray emission from B1055-52 is due to initial cooling then the inferred radius for the neutron star at $D = 1.53$ kpc exceeds 30 km (Ögelman 1995) - a value hardly acceptable from the theoretical point of view. In the case of Geminga, its inferred luminosity drops by a factor of ~ 2.8 relative to the value used by Nel et al. due to a newly determined HST parallax distance of 157 pc (Caraveo et al. 1996), instead of $D = 250$ pc. Fig. 1 presents the inferred *EGRET* luminosities versus model predictions of Harding (1981), with Geminga, and B1055-52 points corrected for $D = 157$ pc, and $\gamma = 1.59$, respectively. Generally, the agreement between theory and observations looks quite satisfactory, even though the Crab pulsar visibly deviates from the trend predicted by Harding (1981).

Arons (1996) presented a simple argument against all models which offer a functional relation for L_γ roughly similar to $L_\gamma \propto B/P^2$, by plotting the voltage ($\sim B/P^2$) available for particles, against the gamma-ray luminosity $L_\gamma(> 100$ MeV) for six *EGRET* pulsars. An extrapolation of the resulting trend towards low values of B/P^2 leads to L_γ exceeding L_{sd} below $\sim 10^{14}$ Volts. Since L_γ must never exceed L_{sd} , this special value of voltage defines then 'an empirical gamma-ray death line' on $P - \dot{P}$ diagram (or on $Voltage - P$ diagram, as originally presented by Arons). It is hard to reconcile such a line with the observed death line for radio emission, which corresponds to $\sim 10^{12}$ Volts. The effect was known already earlier, when polar cap models of Buccheri et al.(1978) and Harding (1981) had been introduced. In the latter model, for a pulsar with $\dot{P} \approx 10^{-15} \text{ s s}^{-1}$, its L_γ would reach L_{sd} at a characteristic age equal to 3×10^7 years (Harding 1981).

Below we propose a polar cap model which is free of the two problems discussed above. This model reproduces gamma-ray luminosities inferred for seven observed pulsars. At the same time it avoids the problem of the empirical gamma-ray death line of Arons (1996), and it relaxes the upper limits' constraints of Nel et al. (1996), especially for old classical pulsars, and millisecond pulsars. In Section 2 we start with recalling the model for total power contained in outflowing particles, which refers directly to the relation analysed by Arons (1996). Then we present arguments for summing all available *CGRO* data in order to get a better

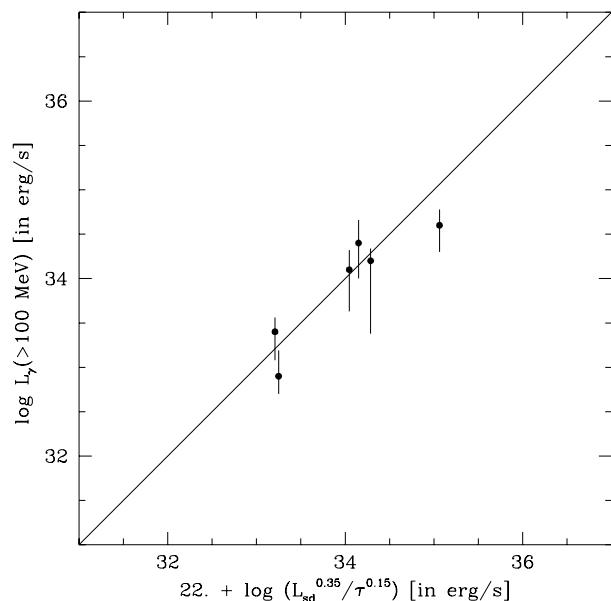


Figure 1. Gamma-ray luminosity above 100 MeV for 6 *EGRET* sources is plotted against predictions of the polar cap model of Harding (1981). The normalization factor is arbitrary; $\tau = P/2\dot{P}$ is a characteristic age expressed in [yr]. (Note: The Crab pulsar is the first dot from the right.) Bars indicate uncertainties in L_γ arising from uncertainties in distance and flux. In the case of Vela (next to Crab) the lower distance limit was extended down to 200 pc to conform to recent estimates based on X-ray and gamma-ray observations of the Vela SNR (400 ± 200 pc after Aschenbach et al.1995 and $\lesssim 350$ pc after Oberlack et al.1994, respectively).

start for a modified polar cap model rather than using the *EGRET* data alone. Section 3 contains a description of our model, and its reference to existing information on gamma-rays from pulsars. Summary and comments are in Section 4; it contains also the ranking of pulsars with the highest gamma-ray fluxes resulting from our model.

2 SIMPLE MODELS VS. *CGRO* DATA

Though *EGRET* has been far more successful than other *CGRO* instruments in detecting pulsars, this does not mean that pulsars' gamma-ray emission above 100 MeV dominates energetically over gamma-ray emission from lower energy bands. In the case of the Crab pulsar most of the energy output occurs within the *COMPTEL* and *OSSE* energy ranges (e.g. Fierro 1995). In the extreme case of B1509-58 there is only *OSSE* detection. Early positive reports from the *COMPTEL* team (Carramiñana et al. 1995) have not been confirmed (Kuiper 1996), and *EGRET* put only upper limits for the source (Thompson et al. 1994). Luminosities listed in Table 1 were inferred from phase-averaged fluxes assuming beaming solid angle of gamma-ray emission Ω_γ equal 1 steradian. For 3 objects (Crab, Vela, and B1951+32) detected with more than one instrument, we can also construct a sum of inferred luminosities (ignoring possible changes of a beaming angle with energy range), to get an estimate of 'total' gamma-ray luminosity. For the remaining 4 pulsars we will use their luminosities in the *EGRET* energy range as 'total'. The values of 'total' gamma-ray luminosities are shown in the last column of Table 1.

Let us now compare these 'total' gamma-ray luminosities with the simplest possible phenomenological polar cap model. According to this model, gamma-ray luminosity L_γ is proportional to a power contained in outflowing primary electrons $L_{\text{particles}}$, which in turn is proportional to a product of primary electron energy E_0 , a surface area of canonical polar cap $A_{\text{pc}} \approx \pi R_{\text{pc}}^2 \propto 1/P$, and a Goldreich-Julian flux $\dot{n}_{\text{GJ}} \propto B/P$ (Goldreich & Julian 1969) of outflowing primary electrons:

$$L_\gamma \propto L_{\text{particles}} \propto E_0 \cdot \dot{n}_{\text{GJ}} \cdot A_{\text{pc}}. \quad (2)$$

Assuming $E_0 = \text{const.}$ for all objects one obtains

$$L_\gamma \propto L_{\text{particles}} \propto B/P^2 \propto L_{\text{sd}}^{1/2}. \quad (3)$$

(Note: The model for $L_{\text{particles}}$ from equation (3) was actually a starting point in the work of Harding 1981, who assumed $E_0 = 10^{13} \text{eV}$ and whose objective was to find a prescription for $L_\gamma (> 100 \text{ MeV})$. We shall return to this point in the next section.)

Figure 2 shows how the relation of equation (3) compares with observations. The normalization factor ($C = 10^{16}$) has been chosen to obtain the best 'by eye' fit. The overall agreement looks quite impressive. There is a substantial improvement for Crab comparing to Figure 1 due to significant contributions from *OSSE* and *COMPTEL* data. Moreover, B1509-58 adds up smoothly to six *EGRET* pulsars. The same functional relation, but for *EGRET* points only, has been considered by Arons (1996) (see previous section).

The relation $L_\gamma = 10^{16} L_{\text{sd}}^{1/2} [\text{erg s}^{-1}]$ presented in Fig.2, cannot hold for all radio pulsars. It leads formally to L_γ reaching L_{sd} at $10^{32} \text{ erg s}^{-1}$ (which corresponds to the Arons' empirical gamma-ray death line), whereas pulsars are observed down to $L_{\text{sd}} \simeq 10^{30} \text{ erg s}^{-1}$. Clearly, pulsar models which predict L_γ as a simple combination of B and P , require some revision.

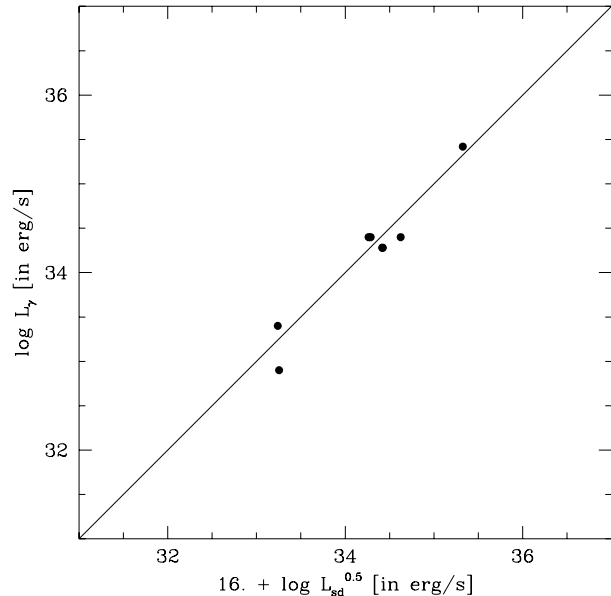


Figure 2. 'Total' gamma-ray luminosity L_γ for all seven *CGRO* sources, inferred from *EGRET*, *COMPTEL*, and *OSSE* observations (wherever available - see Table 1.) are compared with a simple model (equation 3) discussed in Section 2. (Note: B1951+32 and B1706-44 practically coincide. The dot lying at the upper right part of the diagonal represents the Crab pulsar.)

3 HOW DO ELECTRON-POSITRON PAIRS CONTRIBUTE TO GAMMA-RAYS

According to the model of Daugherty & Harding 1982 (DH82) primary electrons are accelerated along open magnetic field lines to high energies ($\sim 10^{13} \text{eV}$) due to rotation-induced electric field. The model assumes a dipolar structure of the magnetic field. Curvature photons emitted by primary electrons are absorbed by magnetic field with subsequent creation of electron-positron pairs (Sturrock pairs). These pairs cool off instantly via synchrotron radiation. Synchrotron photons may lead to further pair creation. Electromagnetic cascades propagating in pulsar's magnetic field may be very rich, with several subsequent generations of pairs and photons.

Numerical treatment of electromagnetic cascades initiated by primary electrons above polar cap, and propagating across the magnetosphere (DH82) does not include effects of possible acceleration of Sturrock pairs. The only contribution from pairs to gamma-rays taken into account is due to synchrotron emission of created pairs. The pairs themselves do not accelerate, and subsequently - do not contribute to the curvature radiation. Such simplification is usually justified by arguing that an appearance of conductive plasma above some height effectively leads to a screening of electric field parallel to local magnetic field lines. If, however, the density of created pairs is lower than the local corotation plasma density, the electrons from pairs will be subject to further acceleration (whereas positrons will be decelerated; eventually some of them will be stopped and reversed towards the stellar surface). In the context of polar cap mod-

els developed by Daugherty & Harding (1982, 1994, 1996) it became clear that potential contribution to gamma-rays from pairs might be necessary to account for the observed gamma-ray fluxes.

If these secondary particles are indeed subject to effective acceleration at significant altitudes above polar cap surface, e.g. at heights of several NS radii (Daugherty & Harding 1996), the resulting beaming angles of gamma-ray emission Ω_γ will be wider than those measured at the polar cap surface. The requirement for “nearly aligned rotators” (Dermer & Sturmer 1994, Daugherty & Harding 1994), necessary to explain large duty cycles of gamma-ray emission, might be then relaxed. [Note: Relaxing the assumption about small inclination angles between the rotation and magnetic axes may be inevitable on observational grounds. Inclination estimates carried out by Lyne & Manchester (1988), and Rankin (1990) show that in many pulsars inclination angles are large indeed. However, mutual comparison of these results shows that they are in agreement only for small inclination angles ($\lesssim 40$ deg), and there is no correlation if either estimate is larger than this value (Miller & Hamilton 1993).] Hereafter we will assume that for all pulsars $\Omega_\gamma = 1$ sr (corresponding to opening angles of ~ 30 degrees).

Suppose, that the secondary particles, which we assume to be created as described in the model of DH82, do participate in the gamma-ray production similarly as the primary electrons do. In the spirit of equations (2) and (3), we propose a following prescription for L_γ :

$$L_\gamma = C \cdot n_\pm \cdot E_\pm \cdot L_{\text{sd}}^{1/2}, \quad (4)$$

where n_\pm is a number of created pairs e^\pm per primary electron, and E_\pm is a characteristic energy attained by particles due to acceleration. The normalization constant C will be determined by fitting the observations. We will assume that E_\pm achieved by secondary particles is similar to the energy attained by primary electrons E_0 , i.e. $E_\pm \simeq E_0$.

We begin with making a choice for the value of E_0 , since it is this parameter which, along with B and P , will determine the number of pairs n_\pm created per primary electron. The analytical fit of Harding (1981) for L_γ above 100 MeV, which gained so much popularity in testing her polar cap model against *EGRET* observations was obtained from numerical simulations performed for a fixed value of primary electron energy $E_0 = 10^{13}$ eV. Originally, this energy has been chosen to make the best spectral fits above 100 MeV for *COS-B* data of Crab and Vela. However, such assumption about E_0 is not possible throughout the entire pulsar’s lifetime because the energy of outgoing electrons is subject to twofold limitation (e.g. Sturrock 1971): there is an absolute upper limit

$$E_W = 1.2 \times 10^7 B_{12} P^{-2} \text{ [MeV]} \quad (5)$$

($B_{12} = B/10^{12}$ G, period P is in [s]) set by potential drop across the polar cap, and a maximum value

$$E_{\text{max}} = 4.6 \times 10^7 B_{12}^{1/4} P^{-1/8} \text{ [MeV]} \quad (6)$$

set up by curvature cooling in purely dipolar magnetic field. The energy E_0 of primary electrons must conform to one of these two limits (whichever comes first) as the pulsar is slowing down, since both E_W and E_{max} decrease as P increases. In consequence, the prescription for L_γ (> 100 MeV)

of Harding (1981) should not be treated as accurate everywhere.

Moreover, accelerating electrons should cross threshold energy

$$E_{\text{min}} = 1.2 \times 10^7 B_{12}^{-1/3} P^{1/3} \text{ [MeV]} \quad (7)$$

required for pair creation. Whenever E_W falls below E_{min} , a classical pulsar crosses the well known deathline, and enters ‘a graveyard for pulsars’. Another deathline occurs for millisecond pulsars even earlier, when E_{max} falls below E_{min} (Rudak & Ritter 1994).

An ultrarelativistic primary electron, sliding along curved magnetic field line, emits curvature photons which in turn may be converted into e^\pm pairs. The total number of pairs created per electron depends on the local component of magnetic field B perpendicular to the direction of propagation of the photon, on the energy of the electron E_0 , and on the curvature of magnetic field lines. As the primary electron accelerates, its energy E_0 will cross the threshold value E_{min} , thus triggering creation of a first pair. The number of created pairs quickly increases as E_0 exceeds E_{min} . At some point it becomes high enough to make further acceleration of electrons less effective due to screening effects. Instead of fixing E_0 at some specific value we assume thus that electrons may be accelerated up to an energy E_0 satisfying following condition throughout pulsar’s entire lifetime:

$$E_0 = \min\{\zeta \cdot E_{\text{min}}, E_W, E_{\text{max}}\}, \quad (8)$$

where $\zeta > 1$.

The best choice for the value of the parameter ζ was made a posteriori, to reproduce the empirical trend of L_γ for the seven *CGRO* pulsars with similar accuracy as equation (3) does in Fig.2. We found that the range $2 \lesssim \zeta \lesssim 5$ fulfills this requirement. All results presented below are for $\zeta = 2.5$. For E_{min} we preferred to take the numerically obtained values whenever they differed from the analytical approximation (the analytical formulae for E_W , E_{max} , and E_{min} are taken from Rudak & Ritter 1994). We found that the former are consistently smaller by a factor of ~ 1.5 (in most cases) than the latter.

The development of cascades was followed by means of numerical simulations described in DH82. Calculations of number of pairs n_\pm were performed with numerical simulations after choosing P and B , and setting the primary electron energy E_0 according to equation (8). The normalization constant in our model of L_γ (equation 4) was determined by fitting numerical results to the seven detections (the last column of Table 1.). Then we calculated two evolutionary tracks in the $L_\gamma - L_{\text{sd}}$ space for representatives of the classical pulsars (with typical magnetic field strength $B \sim 10^{12}$ G), as well as of the millisecond pulsars ($B \sim 10^9$ G). Both tracks are shown in Fig.3 as solid curves. The upper curve ($B \sim 10^{12}$ G) starts at $L_{\text{sd}} \simeq 10^{39}$ erg s $^{-1}$, nearby Crab, and down to $L_{\text{sd}} \sim 10^{34}$ erg s $^{-1}$ it roughly follows the dashed line, which depicts the relation $L_\gamma = 10^{16} \cdot L_{\text{sd}}^{1/2}$ from Section 2. As L_{sd} decreases, our exemplary classical pulsar enters a region where proximity to pulsar’s death line becomes important. The number of created pairs n_\pm declines constantly as the pulsar slows down, and it starts to decrease dramatically when E_W falls below ζE_{min} , affecting thus E_0 in equation (8).

At the point where $E_W = E_{\text{min}}$, the creation of pairs

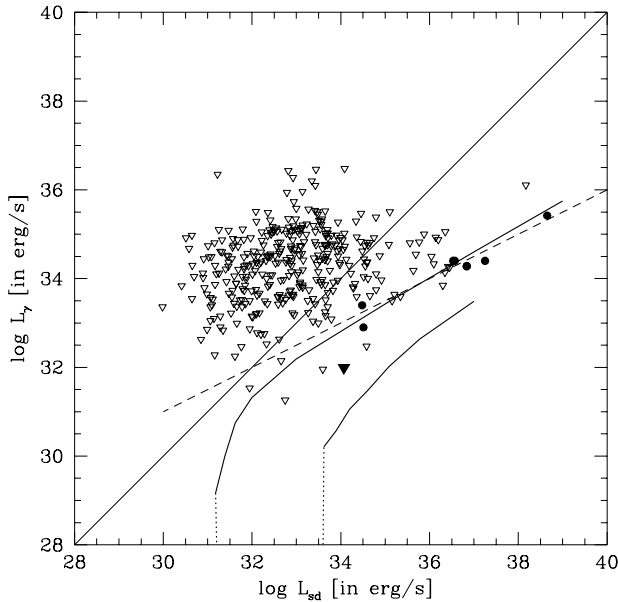


Figure 3. ‘Total’ gamma-ray luminosity is plotted against spin-down luminosity L_{sd} for seven *CGRO* pulsars (filled dots). Open triangles are the *EGRET* upper limits as given by Nel et al.1996 for 350 objects, including seven millisecond pulsars. Filled triangle indicates position of J0437-4715 (after Fierro et al.1995). The dashed line corresponds to $L_\gamma = 10^{16} \cdot L_{sd}^{1/2}$ (see Section 2). The upper solid curve shows the evolutionary track of a pulsar with $B_{pc} = 10^{12}G$, calculated according to eqs. (4) and (8). The lower solid curve shows the evolutionary track for a millisecond pulsar with $B_{pc} = 10^9G$. The evolutionary tracks end up when the objects reach their ‘death points’ in the L_{sd} space (marked with dotted lines).

ceases ($n_{\pm} = 0$) – the pulsar reaches its death line. The exemplary millisecond pulsar ($B_{pc} = 10^9G$) follows the lower solid curve in Fig.3. It starts at $L_{sd} \simeq 10^{37} \text{ erg s}^{-1}$, corresponding to initial period of one millisecond. Unlike the former classical pulsar, it encounters different death line at $L_{sd} \sim 10^{33.5} \text{ erg s}^{-1}$, due to an equality $E_{max} = E_{min}$. The efficiency of pair creation for the millisecond pulsar throughout its lifetime, is significantly lower than for the classical pulsar. Low strength of magnetic field plays a decisive role here, and it cannot be compensated for by faster rotation (and therefore – by smaller curvature radii available). The filled triangle in Fig.3 indicates the upper limit for J0437-4715 set from *EGRET* observations (after Fierro et al.1995). In addition, 350 *EGRET* upper limits (Nel et al. 1996), including seven limits for millisecond pulsars, are shown for comparison. Apart from J0437-4715, four objects with *EGRET* upper limits only are placed clearly below the upper evolutionary track. These are (from right to left): B1046-58, B0656+14, B1929+10, and B0950+08. If the proposed model is correct, these objects should be the best candidates for detection in gamma-rays (but not necessarily in the *EGRET* energy range). B1951+32 and B1509-58, present in the data of Nel et al. (1996), have been replaced with detections (filled dots) by *EGRET* and *OSSE*, respectively.

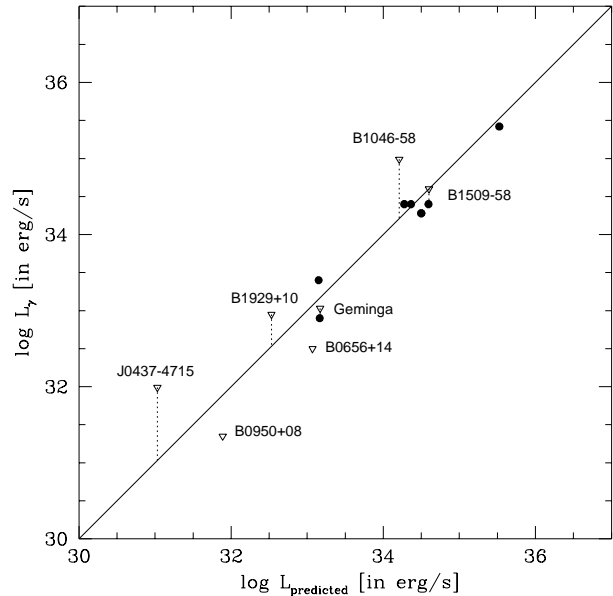


Figure 4. ‘Total’ gamma-ray luminosity is plotted against predicted luminosity, calculated according to eqs. (4) and (8), for seven *CGRO* pulsars (filled dots). Open triangles denote combined *OSSE*, *COMPTEL* and *EGRET* upper limits (wherever available). The continuous diagonal line corresponds to a perfect agreement between predictions and observations.

The comparison of how our model reproduces L_γ for the seven *CGRO* pulsars, along with combined upper limits from *EGRET*, *COMPTEL*, and *OSSE* (from Thompson et al.1994, Fierro et al.1995, Schroeder et al.1995, and Carramiñana et al.1995), wherever available, is shown in Fig.4. In the case of Geminga and B1509-58, the model overestimates the observed L_γ by a factor of ~ 2 . However, existing upper limits from *COMPTEL* and *EGRET*, respectively, improve the agreement. The upper limit for J0437-4715, based on *EGRET* only, is one order of magnitude above the predicted value of L_γ . For four other objects (B1046-58, B0656+14, B1929+10, and B0950+08) the stringent upper limits from *EGRET* differ from the model predictions by no more than a factor of ~ 3 . Moreover, upper limits from *COMPTEL* on B1046-58 and B1929+10 place them on a safe side of the diagonal line of perfect agreement in Fig.4. There is no information available about B0950+08 and B0656+14 from any *COMPTEL* observations.

4 SUMMARY

We have proposed a semi-phenomenological model of gamma-ray emission from pulsars, which is based on polar cap activity triggered by primary electrons. The energy of electrons is only a few times higher than the threshold energy required to induce pair creation in the presence of a dipolar magnetic field, with other restrictions applied when necessary. Electromagnetic cascades induced via curvature radiation were treated in the same way as described by DH82. The important ingredient of the model is the as-

sumption that secondary particles, produced in cascades due to one-photon absorption, contribute to overall gamma-ray emission similarly as primary electrons.

The model was confronted with the gamma-ray luminosities for seven pulsars inferred from available data from *OSSE*, *COMPTEL*, and *EGRET* experiments. We find that the model is consistent with the existing data. Moreover, the model does not lead to any violence of energetics for pulsars with low spin-down luminosity L_{sd} , – the predicted gamma-ray luminosity L_γ never reaches L_{sd} . It avoids, therefore, the problem of ‘an empirical gamma-ray death-line’ as raised by Arons (1996). We also used the *EGRET* archive of 350 upper limits along with *OSSE*, and *COMPTEL* upper limits (published for 15, and 18 pulsars, respectively), to find likely restrictions on the model. We have used some updates with respect to the data used by Nel et al.(1996) in their analysis. The *EGRET* upper limit for B1951+32 was replaced with its detections by *EGRET* (Ramanamurthy et al. 1995), and *COMPTEL* (Kuiper et al.1996a). Similarly, the *EGRET* upper limit for B1509-58 was replaced with *OSSE* detection (Schroeder et al.1995). In the case of B1929+10 the model distance of 170 pc was replaced with 250 pc (see Yancopoulos, Hamilton & Helfand 1994 for detailed arguments).

For a fixed value of L_{sd} , the predicted L_γ depends rather weakly on magnetic field strength B as long as $10^{11}\text{G} \lesssim B \lesssim 10^{13}\text{G}$ (Dyks 1997), especially for pulsars with $L_{sd} \gtrsim 10^{34} \text{ erg s}^{-1}$. That is why all evolutionary tracks calculated for high values of B converge roughly to the asymptotic relation of equation (3) for $L_{sd} \gtrsim 10^{34} \text{ erg s}^{-1}$ (dashed line in Fig.3). Only as B enters the domain of millisecond pulsars ($\sim 10^8 - 10^9\text{G}$), L_γ drops significantly. Therefore, all millisecond pulsars, including J0437-4715, are expected to be very weak gamma-ray emitters regardless of their L_{sd} , and their *EGRET* upper limits alone are still one order of magnitude above our predictions for their gamma-ray luminosities. Qualitatively quite similar behaviour of millisecond pulsars, though for different physical reasons, results from the model of Dermer & Sturmer 1994, which was used explicitly in the context of millisecond pulsars by Sturmer & Dermer 1994. For their luminosity $L_{SD94} = 1.1 \times 10^{10} B^{3/2} P^{-3} \text{ erg s}^{-1}$ of gamma-rays beamed into a solid angle $\Omega_\gamma \approx 1.5 \times 10^{-3} P^{-1} \text{ sr}$ (eqs.2 and 3 of Sturmer & Dermer 1994, respectively), the apparent gamma-ray luminosity for 1 sr can be expressed as

$$L_\gamma = \Omega_\gamma^{-1} L_{SD94} \approx 1.2 \times 10^9 B^{1/2} L_{sd}^{1/2} \text{ erg s}^{-1}, \quad (9)$$

and accordingly for two pulsars with $B = 10^9\text{G}$ and 10^{12}G but identical spin-down luminosity L_{sd} the former object will be placed below the latter one in a diagram like Fig.3. The *EGRET* upper limit for J0437-4715 ($\sim 10^{32} \text{ erg s}^{-1}$) is well above $1.6 \times 10^{30} \text{ erg s}^{-1}$ resulting from equation (9).

Out of several objects in the analysis of Nel et al.(1996), with uncomfortably low *EGRET* upper limits, and contradicting thus the models they discuss, only two are left as a potential threat to our model: B0950+08, and B0656+14. The *EGRET* limits for these two sources are too low to be accommodated by the model. It is encouraging, however, that B0656+14 was reported as a possible *EGRET* source (Ramanamurthy et al. 1996). Both pulsars were on the priority list of *COMPTEL* but with low ranks, and no results are available for them so far. There are no *OSSE* limits available for B0656+14 either. Definitely, B0656+14 deserves more attention as a promising target for gamma-ray experiments

below the energy range of *EGRET*. Its parameters are very similar to those of Geminga and B1055-58. Moreover, all three pulsars are strong X-ray emitters, and are thought to be the best candidates for initial cooling (Ögelman 1995, Becker & Trümper 1997). On the other hand, the combined upper limits available for B1046-58, and B1929+10 (*EGRET*, *COMPTEL*, *OSSE* in both cases) don’t rule out our model.

The upper limits for energy fluxes adopted from Nel et al.(1996), and used also in this work require a word of comment. They were inferred from upper limits for photon fluxes under an assumption that all photon spectra above 100 MeV have a spectral index γ , obeying a trend derived by Thompson et al.(1994) from five *EGRET* pulsars:

$$\gamma = 0.33 \log \tau - 3.08, \quad (10)$$

where the characteristic age of pulsars $\tau = P/2\dot{P}$ is expressed in years. The trend is based essentially on the Crab pulsar ($\gamma = 2.16$, $\tau = 1.3 \times 10^3$) on one side, and on B1055-52 ($\gamma = 1.18$, $\tau = 5.3 \times 10^5$) on the other side. With the new determination of the spectral slope for B1055-58, $\gamma = 1.59$ (Fierro 1995), the prescription for $\gamma(\tau)$ looks questionable. As a consequence, upper limits for L_γ derived for old pulsars, especially for millisecond pulsars, might be somewhat tighter. That would put models discussed by Nel et al.(1996) into even deeper trouble, whereas the model we propose still remains intact.

Pulsars from the database of Taylor, Manchester & Lyne (1993) extended by Taylor et al. (1995), plus Geminga, arranged in a traditional ranking, based just on spin-down fluxes L_{sd}/D^2 , start with Crab and five other gamma-ray pulsars. But then, there is a wide gap (of no gamma-ray detections) before the seventh gamma-ray pulsar, B1055-52, emerges as No.33. The gap contains several millisecond pulsars, with their flagship J0437-4715 taking very high overall position – No.7.

Our ranking of top 30 candidates for gamma-ray emission, arranged by a predicted flux resulting from equations (4) and (8),

$$f_\gamma = C \cdot \frac{n_\pm \cdot E_0 \cdot L_{sd}^{1/2}}{D^2}, \quad (11)$$

is presented in Table 2. The pulsar database of Taylor et al.(1993, 1995) ordered by f_γ starts now with Vela, then goes Crab and Geminga. B1055-52 advances by 13 positions to No.20. The millisecond pulsars (from the gap), including J0437-4715, disappear from the list of ‘Top 30’.

Table 2. Our ranking of top 30 gamma-ray candidates. The seven *CGRO* detections are marked with γ .

	PSR B	PSR J		D [kpc]	L_γ/D^2 [$\text{erg s}^{-1} \text{cm}^{-2}$]
1	0833-45	0835-4510	γ	0.50	0.1302E-07
2	0531+21	0534+2200	γ	2.00	0.8963E-08
3		0633+1746	γ	0.15	0.7308E-08
4	1706-44	1709-4428	γ	1.82	0.6430E-09
5	1929+10	1932+1059		0.25	0.5678E-09
6	0950+08	0953+0755		0.12	0.5646E-09
7	1951+32	1952+3252	γ	2.50	0.4108E-09
8	0656+14	0659+1414		0.76	0.2130E-09
9	1509-58	1513-5908	γ	4.40	0.2080E-09
10	1046-58	1048-5832		2.98	0.1904E-09
11		2043+2740		1.13	0.1653E-09
12	1823-13	1826-1334		4.12	0.1239E-09
13	1800-21	1803-2137		3.94	0.1193E-09
14	0740-28	0742-2822		1.89	0.1143E-09
15	0114+58	0117+5914		2.14	0.1136E-09
16	1757-24	1801-2451		4.61	0.9188E-10
17		1908+0734		0.58	0.9129E-10
18	1727-33	1730-3350		4.24	0.7281E-10
19		0538+2817		1.77	0.6567E-10
20	1055-52	1057-5226	γ	1.53	0.6346E-10
21	0823+26	0826+2637		0.38	0.6209E-10
22		1918+1541		0.68	0.5512E-10
23	0355+54	0358+5413		2.07	0.4791E-10
24	1853+01	1856+0113		3.30	0.4525E-10
25	0450+55	0454+5543		0.79	0.4274E-10
26	1822-09	1825-0935		1.01	0.4079E-10
27	1702-19	1705-1906		1.18	0.3806E-10
28	1133+16	1136+1551		0.27	0.2123E-10
29	0906-17	0908-1739		0.63	0.1433E-10
30	1451-68	1456-6843		0.45	0.8666E-11

ACKNOWLEDGEMENTS

Numerical code used in this work is based on a code originally developed and kindly provided by A.K. Harding. This research has been financed by the KBN grant 2P03D.009.11. We acknowledge useful remarks on the typescript from T. Bulik. We thank the anonymous referee for comments and useful suggestions.

ADDENDUM

Already after submitting our paper for publication Lucien Kuiper pointed to us that the COMPTEL group has found indications for a signal from B0656+14 in the energy interval of 10 – 30 MeV (Hermsen, W., et al., 1997, Proceedings 2nd INTEGRAL Workshop, ESA SP-382, 287).

REFERENCES

Aschenbach, B., Egger, R., Trümper., 1995, *Nature*, 373, 587
Arons J., 1996, *A&AS*, 120, 49
Becker W., Trümper J., 1997, *A&A*, in the press
Buccheri, R., D’Amico, N., Massaro, E., Scarsi, L., 1978, *Nature*, 274, 572
Caraveo P.A., Bignami G.F., Mignani R., Taff L.G., 1996, *ApJ*, 461L, 91

Carramiñana A., Bennett K., Buccheri R., et al. 1995, *A&A*, 304, 258
Daugherty J.K., Harding A.K., 1982, *ApJ*, 252, 337 (DH82)
Daugherty J.K., Harding A.K., 1994, *ApJ*, 429, 325
Daugherty J.K., Harding A.K., 1996, *ApJ*, 458, 278
Dermer C.D., Sturmer S.J., 1994, *ApJ*, 420, L75
Dyks J., 1997, M.Sci. Thesis (UMK Toruń)
Fierro J.M., 1995, Ph.D. Thesis (Stanford University)
Fierro J.M., Arzoumanian Z., Bailes M., Bell J.F., et al., 1995, *ApJ*, 447, 807
Fierro J.M., Bertsch D.L., Brazier K.T.S., et al., 1993, *ApJ*, 413, L27
Goldreich P., Julian W., 1969, *ApJ*, 157, 869
Harding A.K., 1981, *ApJ*, 245, 267
Kuiper L., 1996, contribution to NATO ASI “The Many Faces of Neutron Stars”
Kuiper L., Hermsen W., Bennett K., Carramiñana A., McConnell M., Schönfelder V., 1996a, *A&A*, submitted
Kuiper L., Hermsen W., Bennett K., et al., 1996b, *A&AS*, 120, 73
Lyne, A.G., Manchester, R.N., 1988, *MNRAS*, 234, 477
Michel F.C., 1991, *Theory of Neutron Star Magnetospheres* (University of Chicago Press, Chicago)
Miller, M.C., Hamilton, R.J., 1993, *ApJ*, 411, 298
Nel H.I., Arzoumanian Z., Brazier K.T.S., et al., 1996, *ApJ*, 465, 898
Oberlack, U., Diehl, R., Montmerle, T., et al., 1994, *ApJS*, 92, 433
Ögelman H., 1995, in Proc. NATO ASI “The Lives of Neutron Stars”, ed. A. Alpar, Ü. Kızıloğlu, J. van Paradijs (Dordrecht: Kluwer)
Ramanamurthy P.V., Bertsch D.L., Dingus B.L., et al., 1995, *ApJ*, 447, L109
Ramanamurthy P.V., Fichtel C.E., Kniffen D.A., Sreekumar P., Thompson D.J., 1996, *ApJ*, 458, 755
Rankin, J.M., 1990, *ApJ*, 352, 247
Rudak B., Ritter H., 1994, *MNRAS*, 267, 513
Schroeder P.C., Ulmer M.P., Matz S.M., et al., 1995, *ApJ*, 450, 784
Sturmer, S.J., Dermer, C.D., 1994a, *A&A*, 281, L101
Sturrock P.A., 1971, *ApJ*, 164, 529
Taylor J.H., Cordes J.M., 1993, *ApJ*, 411, 674
Taylor J.H., Manchester R.N., Lyne, A.G., 1993, *ApJS*, 88, 529
Taylor J.H., Manchester R.N., Lyne A.G., Camilo F., 1995, *The Princeton Pulsar Database*
Thompson D.J., Arzoumanian Z., Bertsch D.L., et al., 1994, *ApJ*, 436, 229
Yadigaroglu I.-A., Romani R.W., 1995, *ApJ*, 449, 211
Yancopoulos S., Hamilton T.T., Helfand D.J., 1994, *ApJ*, 429, 832